2-19-2013

Hydroxyl-decorated graphene systems as candidates for organic metal-free ferroelectrics, multiferroics, and high-performance proton battery cathode materials

Menghao Wu
Virginia Commonwealth University

John D. Burton
University of Nebraska-Lincoln, jburton2@unl.edu

Evgeny Y. Tsymbal
University of Nebraska-Lincoln, tsymbal@unl.edu

Xiao Cheng Zeng
University of Nebraska-Lincoln, xzeng1@unl.edu

Purusottam Jena
Virginia Commonwealth University, pjena@vcu.edu

PHYSICAL REVIEW B **87**, 081406(R) (2013)

Hydroxyl-decorated graphene systems as candidates for organic metal-free ferroelectrics, multiferroics, and high-performance proton battery cathode materials

Menghao Wu,[1,2,3,*] J. D. Burton,[3] Evgeny Y. Tsymbal,[3] Xiao Cheng Zeng,[2,*] and Puru Jena[1,*]

[1]*Department of Physics, Virginia Commonwealth University, Richmond, Virginia, 23284, USA*

[2]*Department of Chemistry, University of Nebraska, Lincoln, Nebraska, 68588, USA*

[3]*Department of Physics and Astronomy, University of Nebraska, Lincoln, Nebraska, 68588, USA*

(Received 12 September 2012; revised manuscript received 11 December 2012; published 19 February 2013)

Using a first-principles method we show that graphene based materials, functionalized with hydroxyl groups, constitute a class of multifunctional, lightweight, and nontoxic organic materials with functional properties such as ferroelectricity, multiferroicity, and can be used as proton battery cathode materials. For example, the polarizations of semihydroxylized graphane and graphone, as well as fully hydroxylized graphane, are much higher than any organic ferroelectric materials known to date. Further, hydroxylized graphene nanoribbons with proton vacancies at the end can have much larger dipole moments. They may also be applied as high-capacity cathode materials with a specific capacity that is six times larger than lead-acid batteries and five times that of lithium-ion batteries.

DOI: 10.1103/PhysRevB.87.081406 PACS number(s): 81.05.ue, 31.15.A−, 77.84.−s, 82.47.Cb

It is well known that ferroelectric materials, possessing spontaneous electric polarizations that are switchable under an external electric field, have a wide range of applications in electronics, micromechatronics, and electro-optics.[1] Most of the current ferroelectric materials are based on inorganic elements. Recently, there is considerable interest in synthesizing organic ferroelectric materials since they are light, flexible, and nontoxic. The first ferroelectric crystal, Rochelle salt, which was discovered in 1920,[2] is an organic ferroelectric material containing an organic tartrate ion. At present, the study of ferroelectricity in organic solids has been limited to some well-known polymer ferroelectrics[3] such as polyvinylidene difluoride (PVDF),[4–10] or a few low-molecular-mass compounds such as thiourea,[11] tetrathiafulvalene (TTF) complexes with *p*-bromanil (tetrabromo-*p*-benzoquinone)[12] and *p*-chloranil (tetrachloro-*p*-benzoquinone),[13] croconic acid,[14] and so on. Multiferroicity, i.e., the coexistence of magnetism and ferroelectricity, is even more desirable for constructing multifunctional devices[15,16] where electrical polarization can be controlled by applied magnetic fields and magnetization by applied voltage. Magnetic and electrical ordering, however, requires very different molecular interactions that are hard to incorporate in the same compound. Consequently, there are very few organic multiferroic materials predicted or synthesized at present.[17–19]

In this Rapid Communication, using calculations based on density functional theory, we show that several types of lightweight organic ferroelectric materials with high spontaneous polarizations can be designed by functionalizing graphene with hydroxyl groups. For example, the polarizations of semihydroxylized graphane and graphone as well as fully hydroxylized graphane are, respectively 41.1, 43.7, and 67.7 $\mu C/cm^2$, much higher than any organic ferroelectric materials known to date. In addition, hydroxylized graphone is multiferroic due to the coexistence of ferroelectricity and ferromagnetism. Zigzag graphene nanoribbons decorated with hydroxyl groups also exhibit ferroelectric properties with a large polarization of 27.0 $\mu C/cm^2$. Moreover, proton vacancies at the ends of the ribbons can induce dipole moments that can be reversed by both hopping of protons and the rotation of O–H bonds under an electric field. We also explore their potential as high-capacity cathode materials where we find a specific capacity that is six times larger than lead-acid batteries and five times that of lithium-ion batteries. This study provides pathways to the synthesis of high-performance organic, metal-free ferroelectric, multiferroic, and proton battery cathode materials which have many advantages over conventional ferroelectric materials, such as no spatial constraint, high-temperature performance, directional hydrogen bonds, low dimension, and green fabrication from renewable energy resource such as carbohydrates.

Our starting material, graphene, is a single layer of carbon atoms in a honeycomb lattice, which has attracted considerable attention since it was first isolated experimentally in 2004.[20] Many of its novel physical properties, such as exhibiting a room-temperature quantum Hall effect, massless Dirac fermion behavior, and high electron mobility and coherence have been explored.[20–26] Although pristine graphene is a semimetal and chemically inert, a previous experimental report has shown that it can be chemically converted into a graphane layer (an insulator) by saturating all carbon atoms with atomic hydrogen.[27–30] It has also been theoretically predicted that half-hydrogenated graphene (referred to as graphone) is a magnetic semiconductor.[31] Graphene can also be transformed into a semiconductor by cutting it into rectangular slices, namely, graphene nanoribbons (GNRs). The band gaps of these GNRs depend on the width of the nanoribbons and the crystallographic orientation of the cutting edge.[32–37] Their electronic properties can be further tuned through decorations.[37–40]

Here, we decorate graphane and graphone nanoribbons with hydroxyl groups. Semihydroxylized graphane (SHLGA) is achieved by replacing the H atoms on one side of graphane with –OH groups while fully hydroxylized graphane (HLGA) is achieved by replacing all H atoms with –OH groups. Hydroxylized graphone (HLGO), on the other hand, is achieved by replacing the H atoms on graphone with –OH while the on the other side C atoms retain their dangling bonds. Calculations are carried out using gradient corrected density

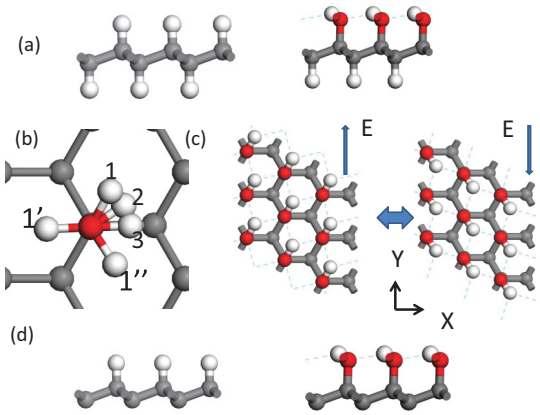

FIG. 1. (Color online) (a) Side view of graphane and SHLGA, (b) different orientations of the hydroxyl group in SHLGA, (c) top view of SHLGA with different polarization orientations, and (d) side view of graphone and HLGO. Gray, white, and red spheres denote C, H, and O atoms, respectively.

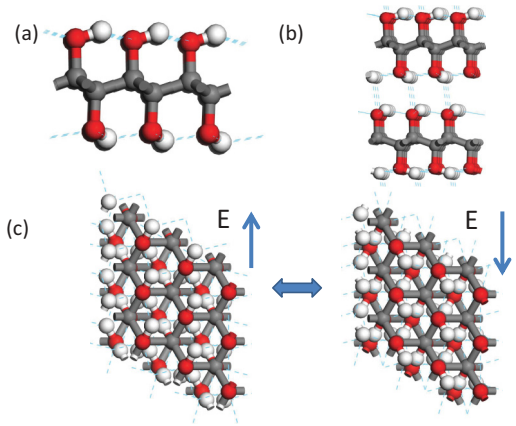

FIG. 2. (Color online) (a) Side view of single-layer HLGA, (b) multilayer HLGA, and (c) top view of multilayer HLGs.

functional theory (DFT-GGA) and the DMOL^3 package.[41,42] The generalized gradient approximation (GGA) in the Perdew-Burke-Ernzerhof (PBE) functional form[43] for the exchange-correlation functional and an all-electron double numerical basis set with a polarized function (DNP) are chosen for the spin-unrestricted DFT computation. The real-space global cutoff radius is set to 4.5 Å. The sizes of the supercell as well as all atomic positions were optimized until the forces were below 0.0002 Ha/Å. The distances between layers in the three-dimensional (3D) bulk structures are also optimized. For electronic band-structure calculations, the Brillouin zone is sampled using a $5 \times 5 \times 3$ k-point grid in the Monkhorst-pack scheme.[44] The PBE-D2 functional of Grimme was used to take into account dispersive forces[45] and the Berry-phase method was employed to evaluate crystalline polarization[46,47] using the Vienna *ab initio* simulation package (VASP).[48–50]

First we consider SHLGA where hydrogen atoms on one side of a graphane layer are replaced by hydroxyl groups, as shown in Fig. 1(a). The average binding energy of every hydrogen atom on graphane is -2.5eV, and during the process of substitution an energy of 0.3 eV is required for every hydroxyl group. The hydrogen atom in an –OH group may occupy positions marked 1, 2, or 3 in Fig. 1(b). According to our calculations, site 1 is the ground state while sites 2 and 3 lie, respectively, 0.042 and 0.055 eV higher in energy. This is understandable as the proton located over the center of a hexagon, as in position 1, can form two hydrogen bonds simultaneously with two O atoms of adjacent –OH groups. In addition, being farther from C atoms, it suffers less repulsion. There are also two other positions, $1'$ and $1''$, which are equivalent to site 1. As the hydrogen atom occupies any one of those sites, the lengths of the covalent O–H and the hydrogen O–H bonds are, respectively, 0.99 and 1.87 Å. In the ground state, there is one hydrogen atom over every carbon hexagon and all the –OH groups point towards one direction, as displayed in Fig. 1(c), making SHLGA a two-dimensional (2D) ferroelectric material with a spontaneous polarization of 2.5×10^{-12} C/cm projected along the Y axis. This ferroelectric polarization is switchable through the rotation of O–H bond under an applied external electric field, with an energy barrier of 0.055 eV per proton. When SHLGAs are stacked layer by layer, we obtain a 3D bulk material with a spontaneous polarization of 41.1 μC/cm^2 projected along the Y direction. This is even larger than that in croconic acid (with the highest known polarization, 21 μC/cm^2, among current organic ferroelectrics)[35] and bulk $BaTiO_3$ (26 μC/cm^2). When a similar substitution of H atoms by –OH groups is performed in graphone (where only one side of the C atoms is saturated with hydrogen) we denote the system as hydroxylized graphone (HLGO), as shown in Fig. 1(d). Stacking of HLGOs layer by layer would require less space, resulting in spontaneous polarization along the Y axis of 43.7 μC/cm^2, which is even larger than that found for SHLGAs. More importantly, the 3D HLGO system is magnetic just as graphone, with a magnetic moment of $2.0\mu_B$ per unit cell (every unit cell contains four carbon atoms in two layers), making HLGO multiferroic.

Figure 2(a) displays the geometry where all the hydrogen atoms in graphane are replaced by hydroxyl groups. We denote this system as a fully hydroxylized graphene sheet (HLGA). When layers of HLGA are stacked periodically, it is energetically favorable for –OH groups to form interlayer hydrogen bonds. Different configurations and relative energies are listed in Fig. S1 in the Supplemental Material,[51] indicating ABAB stacking is favorable in energy. The side and top views of the ground state structures are shown in Figs. 1(b) and 1(c), respectively. We find a spontaneous polarization of 67.7 μC/cm^2 along the Y axis, switchable under an applied electric field. This is almost twice as large as that of the value in bulk SHLGA.

Hydroxylized zigzag-edge graphene nanoribbons (ZGNRs) also exhibit ferroelectricity. According to previous studies,[39,40] an energy of 0.17 eV per edge site is released when every H atom on a pristine ZGNR is substituted by a –OH group. We find that –OH groups decorated on the zigzag edges will form hydrogen bonds with adjacent –OH groups. We find a spontaneous polarization of 0.25 e Å per Å associated with the displacement of protons, switchable through the rotation of the O–H bond along the direction of the ZGNR, as shown in Fig. 3(a). The energy barrier for this rotation is 0.65 eV per –OH group. To achieve the maximum magnitude of ferroelectric

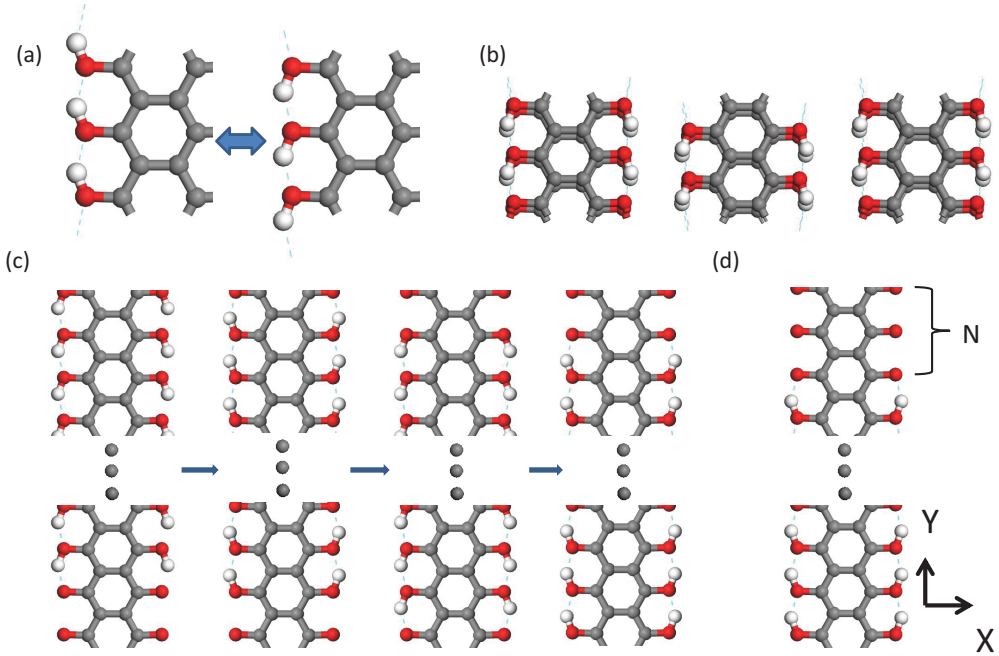

FIG. 3. (Color online) (a) Hydroxylized zigzag edge of ZGNR; (b) bulk crystal of ZGNRs decorated with –OH; ZGNR decorated with –OH with (c) two proton vacancies and (d) N proton vacancies at every edge.

polarization in a crystallized 3D structure, we decorated both edges of the narrowest possible ZGNRs with –OH groups and packed them to form a bulk structure, as shown in Fig. 3(b), yielding a polarization of 27.0 μC/cm^2.

Moreover, if we assume that at the end of every edge of a hydroxylized ZGNR along the Y direction there are two proton vacancies, i.e., two =O bonds [see Fig. 1(c)], the protons will hop and bind to adjacent O atoms, crossing an energy barrier of 0.34 eV under an external electric field along the ZGNR toward the $-Y$ direction. The O–H bond will then rotate to the other side, and H will hop to the last O atom in the end. Here two mechanisms of ferroelectric reversal are clarified: proton hoping and rotation, and the displacements of every proton during hopping and rotation are, respectively, 0.58 and 1.88 Å. The corresponding changes in the dipole moment are, respectively, 1.23 and 1.23 e Å, leading to a switchable polarization of $(1.23 + 1.23 + 1.23)/2 = 1.85\,e$ Å per proton. If there are N proton vacancies at the end of every zigzag edge, as shown in Fig. 3(d), the polarization will be $0.62 + (N - 1)1.23\ e$ Å per proton and will increase linearly with N.

In addition to their giant polarizations, these ferroelectric hydroxylized graphite nanomaterials have many advantages over conventional organic ferroelectric materials such as PVDF. As previously noted:[52] (1) The ferroelectric PVDF family often faces steric hindrance or high energy barriers during switching due to limited intermolecular space, while protons in hydrogen-bonded ferroelectrics can be free to move due to less spatial constraint. (2) The directional preference of hydrogen bonding enables polarity to form spontaneously, while in conventional organic ferroelectrics the tendency for antiparallel molecular aggregations induced by intermolecular dipole-dipole interactions is hard to avoid. (3) The presence of hydroxyl protons tightly bounded to oxygen guards against thermal agitation, resulting in robust high-temperature ferroelectricity. We performed a quantum molecular dynamics simulation on SHLGA and found it still in good ferroelectric order at 500 K, as displayed in Fig. S3 in the Supplemental Material.[51] Moreover, they can exhibit ferroelectricity in low dimensions (2D for SHLGA and HLGO, 1D for hydroxylized ZGNR), while those composed of small molecules[11–14] can only exhibit ferroelectricity in 3D bulk crystal. In addition it is also likely that the systems we propose here can be fabricated from graphite oxide or common carbohydrates such as sugars as they only contain C, H, and O, thus enabling green synthesis

Equally important, we also find that the above hydroxyl-decorated graphene systems may serve as ideal cathode materials for use in rechargeable proton batteries because of the high capacity of protons. As shown in Fig. 4(a), when half of

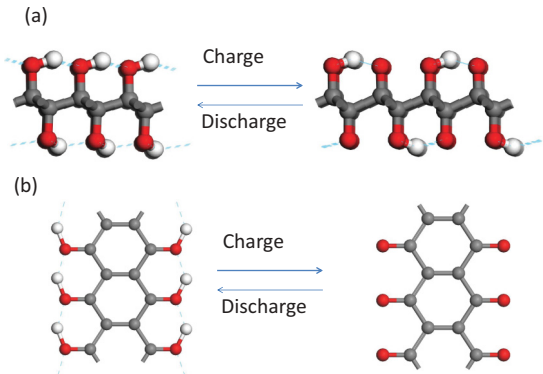

FIG. 4. (Color online) Intercalation and deintercalation of cathode materials based on (a) HLGA and (b) ZGNR decorated with –OH.

the protons in HLG are released, the remaining graphene oxide structure is still stable, so a HLGA has a high specific capacity of 461 mA h/g. During deintercalation, the system would gain 3.40 eV per proton on the average, thus making it suitable as a cathode material. For a ZGNR decorated with –OH groups, all the protons can be released, leaving the remaining system as shown in Fig. 4(b), giving rise to a specific capacity of 669 mA h/g, and making it a suitable cathode material since the system gains, on the average, 3.35 eV per proton during deintercalation. Here the volume should change little during the charging and discharging process by small protons. More importantly, the highest specific capacity we obtained is almost *six* times the highest theoretical value of the lead-acid battery (PbO_2, 111 mA h/g), as well as *five* times that of lithium-ion batteries ($LiCoO_2$, 140 mA h/g). In addition, these potential organic cathode materials can be produced from renewable resources, thus avoiding the pollution caused by the toxic transition-metal atoms in current rechargeable batteries.[53–55]

In conclusion, using first-principles calculations we predict that hydroxylized graphene systems have the potential to serve as environmentally friendly organic ferroelectric materials that are simultaneously lightweight and nontoxic. We find that semihydroxylized graphane, hydroxylized graphone, and fully hydroxylized graphane have large polarizations of, respectively, 41.1, 43.7, and 67.7 $\mu C/cm^2$. In addition, semihydroxylized graphone is multiferroic. ZGNRs decorated with –OH groups are also shown to be ferroelectric with a polarization of 27.0 $\mu C/cm^2$. With proton vacancies at the ends of the edges, much larger dipole moments can be induced by longer displacements of protons. We also summarize many other merits compared with conventional organic ferroelectrics. Finally, we show that these systems have the potential as high-capacity cathode materials with a specific capacity that is *six* times that of current lead-acid batteries and *five* times that of lithium-ion batteries. This study provides pathways to the synthesis of high-performance organic, metal-free, ferroelectric, multiferroic, and proton battery cathode materials which have many advantages over conventional ferroelectric materials, such as no spatial constraint, high-temperature performance, directional hydrogen bonds, low dimension, and green fabrication from renewable energy resource such as carbohydrates. They may also be fabricated from graphene oxide or unzipping of carbon nanotubes by oxygen[56] in experiment. In a very recent experimental paper[57] the discovery of ferroelectricity of graphene oxides has been reported. This is attributed to the 1D hydrogen-bond chains by hydroxyls and supports our predictions.

This research was supported by the National Science Foundation through the Nebraska EPSCoR (NSF Grant No. EPS-1010674) and the Nebraska MRSEC (NSF Grant No. DMR-0820521). P.J. acknowledges partial support by the Department of Energy. Computations were performed at the Department of Chemistry, University of Nebraska-Lincoln.

*Corresponding author: mwu2@vcu.edu, xzeng1@unl.edu, pjena@vcu.edu

[1] M. Lines and A. Glass, *Principles and Applications of Ferroelectrics and Related Materials* (Clarendon, Oxford, 1997).
[2] J. Valasek, Phys. Rev. **15**, 537 (1920).
[3] H. Sachio and T. Yoshinori, Nat. Mater. **7**, 357 (2008).
[4] M. Poulsen and S. Ducharme, IEEE Trans. Dielectr. Electr. Insul. **17**, 1028 (2010).
[5] Y. Yasuhiro and H. Tadokoro, Macromolecules **13**, 1318 (1980).
[6] *Encyclopedia of Smart Materials*, edited by Q. Zhang, V. Bharti, G. Kavarnos, and M. Schwartz (Wiley, New York, 2002), Vols. 1 and 2, pp. 807–825.
[7] A. V. Bune *et al.*, Nature (London) **391**, 874 (1998).
[8] S. Tasaka and S. Miyata, Ferroelectrics **32**, 17 (1981).
[9] J. M. López-Encarnación, J. D. Burton, E. Y. Tsymbal, and J. P. Velev, Nano Lett. **11**, 599 (2011).
[10] Y. Pei and X. C. Zeng, J. Appl. Phys. **109**, 093514 (2011).
[11] G. J. Goldsmith and J. G. White, J. Chem. Phys. **31**, 1175 (1959).
[12] Y. Tokura, S. Koshihara, Y. Iwasa, H. Okamoto, T. Komatsu, T. Koda, N. Iwasawa, and G. Saito, Phys. Rev. Lett. **63**, 2405 (1989).
[13] H. Okamoto, T. Mitani, Y. Tokura, S. Koshihara, T. Komatsu, Y. Iwasa, T. Koda, and G. Saito, Phys. Rev. B **43**, 8224 (1991).
[14] S. Horiuchi *et al.*, Nature (London) **463**, 789 (2010).
[15] S. Cheong and M. Mostovoy, Nat. Mater. **6**, 13 (2007).
[16] R. Ramesh and N. A. Spaldin, Nat. Mater. **6**, 21 (2007).
[17] G. Giovannetti, S. Kumar, A. Stroppa, J. vanden Brink, and S. Picozzi, Phys. Rev. Lett. **103**, 266401 (2009).
[18] M. Wu, J. Burton, E. Tsymbal, X. C. Zeng, and P. Jena, J. Am. Chem. Soc. **134**, 14423 (2012)
[19] F. Kagawa, S. Horiuchi, M. Tokunaga, J. Fujioka, and Y. Tokura, Nat. Phys. **6**, 169 (2010).
[20] K. S. Novoselov *et al.*, Science **306**, 666 (2004).
[21] K. S. Novoselov, A. K. Geim, S. V. Morozov, D. Jiang, I. V. Katsnelson, I. V. Grigorieva, S. V. Dubonos, and A. A. Firsov, Nature (London) **438**, 197 (2005).
[22] M. L. Katsnelson, K. S. Novoselov, and A. K. Geim, Nat. Phys. **2**, 620 (2006).
[23] A. H. Castro Neto, F. Guinea, and N. M. R. Peres, Phys. World **19**, 33 (2006).
[24] A. K. Geim and K. S. Novoselov, Nat. Mater. **6**, 183 (2007).
[25] Y. Zheng and T. Ando, Phys. Rev. B **65**, 245420 (2002).
[26] Y. Zhang, Y. W. Tan, H. L. Stormer, and P. Kim, Nature (London) **438**, 201 (2005).
[27] S. Ryu, M. Y. Han, J. Maultzsch, T. F. Heinz, P. Kim, M. L. Steigerwald, and L. E. Brus, Nano Lett. **8**, 4597 (2008).
[28] D. C. Elias *et al.*, Science **323**, 610 (2009).
[29] J. O. Sofo, A. S. Chaudhari, and G. D. Barber, Phys. Rev. B **75**, 153401 (2007).
[30] D. W. Boukhvalov, M. I. Katsnelson, and A. I. Lichtenstein, Phys. Rev. B **77**, 035427 (2008).
[31] J. Zhou, Q. Wang, Q. Sun, X. S. Chen, Y. Kawazoe, and P. Jena, Nano Lett. **9**, 3867 (2009).
[32] M. Fujita, K. Wakabayashi, K. Nakada, and K. J. Kusakabe, J. Phys. Soc. Jpn. **65**, 1920 (1996).

[33]K. Nakada, M. Fujita, G. Dresselhaus, and M. S. Dresselhaus, Phys. Rev. B **54**,17954 (1996).
[34]K. Kusakabe and M. Maruyama, Phys. Rev. B **67**, 092406 (2003).
[35]L. Pisani, J. A. Chan, B. Montanari, and N. M. Harrison, Phys. Rev. B **75**, 064418 (2007).
[36]O. Hod, V. Barone, and G. E. Scuseria, Phys. Rev. B **77**, 035411 (2008).
[37]E. J. Kan, Z. Li, J. L. Yang, and J. G. Hou, J. Am. Chem. Soc. **130**, 4224 (2008).
[38]M. Wu, P. Pei, and X. C. Zeng, J. Am. Chem. Soc. **132**, 5554 (2010).
[39]M. Wu, X. Wu, Y. Gao, and X. C. Zeng, Appl. Phys. Lett. **94**, 22311 (2009).
[40]M. Wu, X. Wu, and X. C. Zeng, J. Phys. Chem. C **114**, 3937 (2010).
[41]B. Delley, J. Chem. Phys. **92**, 508 (1990).
[42]B. Delley, J. Chem. Phys. **113**, 7756 (2000).
[43]J. P. Perdew, K. Burke, and M. Ernzerhof, Phys. Rev. Lett. **77**, 3865 (1996).
[44]H. J. Monkhorst and J. D. Pack, Phys. Rev. B **13**, 5188 (1976).
[45]S. Grimme, J. Comput. Chem. Soc. **27**, 1787 (2006).
[46]R. D. King-Smith and D. Vanderbilt, Phys. Rev. B **47**, 1651 (1993).
[47]R. Resta, M. Posternak, and A. Baldereschi, Phys. Rev. Lett. **70**, 1010 (1993).
[48]G. Kresse and J. Hafner, Phys. Rev. B **47**, 558 (1993).
[49]G. Kresse and J. Furthmuller, Phys. Rev. B **54**, 11169 (1996).
[50]G. Kresse and D. Joubert, Phys. Rev. B **59**, 1758 (1999).
[51]See Supplemental Material at http://link.aps.org/supplemental/10.1103/PhysRevB.87.081406 for different configurations of hydroxylized graphene systems and snapshot of molecular dynamics simulation on SHLGA.
[52]S. Horiuchi, R. Kumai, and Y. Tokura, Adv. Mater. **23**, 2098 (2011).
[53]A. Manthiram, J. Phys. Chem. Lett. **2**, 176 (2011).
[54]M. Armand and J. M. Tarascon, Nature (London) **451**, 652 (2008).
[55]B. Kang and G. Ceder, Nature (London) **458**, 190 (2009).
[56]D. V. Kosynkin *et al.*, Nature (London) **458**, 872 (2009).
[57]X. Kong and Q. Chen, Acta Chim. Sin. (2013), http://sioc-journal.cn/Jwk_hxxb/CN/10.6023/A12090707.